EXPERIMENTAL AND MODELLING STUDY OF THE ANISOTROPY OF TEMPERATURE DISSIPATION DOWNSTREAM OF A HEATED LINE SOURCE

Lionel Rosset, Pierre Paranthoën,
Jean-Claude Lecordier and Michel Gonzalez
UMR 6614/CORIA, CNRS
76821 Mont-Saint-Aignan, France
Pierre.Paranthoen@coria.fr, Michel.Gonzalez@coria.fr

ABSTRACT

Anisotropic injection of a scalar in a turbulent medium is realized by heating a line source in two kinds of flow namely, a turbulent boundary layer and a turbulent plane jet. In the conditions of those experiments, temperature can be considered as a passive scalar advected by the flow. The three instantaneous temperature gradients are measured. The experimental data show that the second-order moments of the temperature gradients are highly anisotropic near the line source. This anisotropy relaxes with downstream distance. A model representing the evolution of the variance of the temperature gradients is also proposed and enables us to interpret the data and to derive the time scale of the return to isotropy at the level of temperature dissipation.

INTRODUCTION

Better understanding of small-scale mixing needs detailed investigations of the statistics of scalar gradients. In this respect, a number of questions are still unanswered. Specially, the possible contamination of the smallest scales by large-scale properties has motivated the examination of widely accepted concepts such as the local isotropy (Warhaft, 2000). As a matter of fact, violation of this basic assumption has been proved for passive scalars in shear flows (Krishnamoorthy and Antonia, 1987; Sreenivasan, 1991). Experiments have furthermore revealed that in isotropic turbulence, the small-scale anisotropy of a passive scalar experiencing large-scale anisotropic forcing apparently holds with increasing Reynolds number (Tong and Warhaft, 1994).

Most of the previous studies have been specially focused on the estimate of the possible small-scale anisotropy as well as on the way in which large-scale features can be felt down to dissipative scales (Pumir, 1994; Tong and Warhaft, 1994). However, a little is known of mechanims hindering anisotropy at the level of dissipation. From the exact equations for the second-order moments of scalar derivatives, it can be inferred that only stretching and/or molecular dissipation are likely to promote this return to isotropy (Gonzalez, 2000). The precise scenario, however, remains unclear.

The present study differs from previous ones in that it addresses the case in which anisotropy is directly imposed at the small scales of a scalar field. This is realized by heating a small-diameter wire placed, successively, in a turbulent boundary layer and a turbulent plane jet; the geometry of the heated line implies that the temperature field has a high small-scale anisotropy in the near field of the source. The temperature signal is measured by means of cold-wire thermometry. The Taylor's hypothesis is used to derive the instantaneous temperature gradient in the flow direction while the other two instantaneous gradients are measured by using a double cold-wire probe. A model describing the longitudinal evolution of the second-order moments of these gradients at the source height is also devised and used to analyze the experimental data paying particular attention to the return-to-isotropy phenomenon.

EXPERIMENTAL CONDITIONS

The experimental setting up in the turbulent boundary layer and the turbulent plane jet is displayed in Figures 1 and 2 respectively. The free stream velocity of the turbulent boundary layer is 6.4 $m.s^{-1}$ and the boundary layer thickness at the source location is $\delta = 63$ mm. The turbulent jet exits normally to an end plate from a slit of width $b = 15$ mm and span 15 cm; its velocity at the nozzle exit is maintained at 6.7 $m.s^{-1}$.

The heated line source is a Kanthal wire (diameter $d_s = 0.09$ mm). It is heated by Joule effect and tensioned laterally across the flow. The effective Reynolds number of the wire, Re, is just smaller than the critical vortex shedding Reynolds number. The ratio Gr/Re^2 where Gr is the Grashof number defined as $Gr = g\beta\Delta\theta d_s^3/\nu$, is about 2 10^{-4} and thereby low enough to consider heat as a passive contaminant. In the previous definition, g is the acceleration due to gravity and β the temperature coefficient for volume expansion. The Reynolds number of the wire is $Re = U_s d_s/\nu(T_{eff})$; U_s is the mean longitudinal velocity at the source location and ν, the kinematic viscosity, is taken at the temperature T_{eff} defined as $T_{eff} = T_u + 0.24\,\Delta\theta$ where $\Delta\theta$ is the difference between the temperature of the line source and the temperature T_u of the upstream flow (Dumouchel et al., 1998). In the boundary layer, the source is located at height $h_s = 19$ mm that is, $h_s/\delta = 0.3$. In the plane jet, it is placed on the jet axis, at $\Delta x_s = 10$ cm from the nozzle ($\Delta x_s/b = 6.7$). The characteristics of each flow at the source location are given in table 1.

The velocity field is measured using Pt-Rh 10%, 2.5 μm diameter X-hot wires at an overheat ratio 1.5 with DISA 55M constant temperature bridges. Temperature fluctuations are measured with a single Pt-Rh 10%, 0.7 μm diameter cold wire, operated at 0.1 mA. Measurements of the dissipation rate of temperature fluctuations, ϵ_θ ($\epsilon_\theta = \epsilon_{\theta_x} + \epsilon_{\theta_y} + \epsilon_{\theta_z}$; $\epsilon_{\theta_x} = D\overline{(\partial\theta'/\partial x)^2}$, ...where D is the thermal diffusivity) are realized using a two-wire probe consisting of two parallel cold wires. The latter are 0.5 mm long and their diameter is 0.7 μm. The minimal distance between the wires is 0.2 mm. The contribution ϵ_{θ_x} is measured from time correlation functions, using the Taylor's hypothesis; ϵ_{θ_y} and ϵ_{θ_z} are measured from spatial temperature correlation functions for small separations along y and z directions. Close to the source, ϵ_{θ_y} and ϵ_{θ_z} are obtained using an extended parabolic method (Rosset et al., 2000) inspired from the one Aronson and Löfdahl (1993) used for velocity measurements.

	Plane jet	Boundary layer
U_s	6.1 $m.s^{-1}$	5.0 $m.s^{-1}$
$\overline{u'^2}^{1/2}/U_s$	0.15	0.08
$\overline{v'^2}^{1/2}/U_s$	0.17	0.05
$k = 0.75(\overline{u'^2} + \overline{v'^2})$	1.46 $m^2.s^{-2}$	0.17 $m^2.s^{-2}$
$\epsilon = 15\nu U_s^{-2}\overline{(\partial u'/\partial t)^2}$	22 $m^2.s^{-3}$	1.55 $m^2.s^{-3}$
$\eta = (\nu^3/\epsilon)^{1/4}$	0.11 mm	0.22 mm
$U_s/(2\pi\eta)$	8.8 kHz	3.7 kHz
$\lambda = (15\nu\overline{u'^2}/\epsilon)^{1/2}$	3 mm	4.8 mm
$Re_\lambda = \overline{u'^2}^{1/2}\lambda/\nu$	190	130
Integral time scale of u	1 ms	4.5 ms
Integral time scale of v	0.9 ms	1.3 ms
k/ϵ	66 ms	110 ms

Table 1: Flow data at the source location

MODELLING

The analysis is restricted to the longitudinal evolution of the thermal field at the source height, in the region where the budget of temperature variance, $\overline{\theta'^2}$, is governed by convection and dissipation (Raupach and Legg, 1983; Rosset, 2000). In this regime, $\overline{\theta'^2}$ decays according to:

$$\overline{u}\frac{\partial\overline{\theta'^2}}{\partial x} = -2\epsilon_\theta \qquad (1)$$

The observed power-law decay of $\overline{\theta'^2}$ with downstream distance (Rosset, 2000) furthermore suggests that the ϵ_θ equation is:

$$\overline{u}\frac{\partial\epsilon_\theta}{\partial x} = -\psi_\theta\frac{\epsilon_\theta^2}{\overline{\theta'^2}} \qquad (2)$$

with ψ_θ being constant. It is easy to show that Eq. (2) is equivalent to the model of Sykes et al. (1984) describing the decay of ϵ_θ in the inertial regime, in stationary turbulence (Fall, 1997). Then, following Thomson (1997), ϵ_θ can in this case be parametrized as $\epsilon_\theta = 3\zeta\overline{\theta'^2}/4t$ where ζ indicates the dimensionality of the source ($\zeta = 1$, 2 or 3 for, respectively, an instantaneous area, line or point source). From the previous expression (with $t = x/\overline{u}$) and Eqs. (1) and (2), it follows that $\psi_\theta = (6\zeta + 4)/3\zeta$. Provided the turbulence intensity is not too large, a continuous line source can be considered as equivalent to an instantaneous area source (Thomson, 1997) which implies $\zeta = 1$ and hence $\psi_\theta = 10/3$.

We now assume a convection/dissipation budget for the components $\mathcal{E}_{ij} = 2D\overline{(\partial\theta'/\partial x_i)(\partial\theta'/\partial x_j)}$ ($\mathcal{E}_{11} = 2\epsilon_{\theta_x}$, $\mathcal{E}_{22} = 2\epsilon_{\theta_y}$, $\mathcal{E}_{33} = 2\epsilon_{\theta_z}$; the half trace of $\mathcal{E}$ is nothing but ϵ_θ) and write:

$$\overline{u}\frac{\partial\mathcal{E}_{ij}}{\partial x} = -\frac{2}{3}\psi_\theta\frac{\epsilon_\theta^2}{\overline{\theta'^2}}\delta_{ij} - \alpha_{\mathcal{R}}\left(\mathcal{E}_{ij} - \frac{2}{3}\epsilon_\theta\delta_{ij}\right)\frac{\epsilon_\theta}{\overline{\theta'^2}} \qquad (3)$$

The first term on the right-hand side of Eq. (3) stands for the isotropic dissipation of $\mathcal{E}_{ij}$ (in actual fact, the net dissipation resulting from the difference between the isotropic parts of molecular dissipation and stretching). The second one is a model representing the return to isotropy as a relaxation mechanism acting with the characteristic frequency $\tau_{\mathcal{R}}^{-1} = \alpha_{\mathcal{R}}\epsilon_\theta/\overline{\theta'^2} = \alpha_{\mathcal{R}}\tau_\theta^{-1}/2$ as proposed previously (Gonzalez, 2000). In this model, it is stated that $\alpha_{\mathcal{R}}$ is constant. In particular, $\alpha_{\mathcal{R}}$ is assumed not to depend on the turbulence Reynolds number. Local isotropy would imply $\alpha_{\mathcal{R}}$ to increase with the latter but recent experiments (Tong and Warhaft, 1994) have shown that anisotropy at the dissipative scales of a scalar field apparently does not relax when the turbulence Reynolds number is increased which lends support to the idea that $\alpha_{\mathcal{R}}$ might be, at most, slightly Reynolds number dependent.

RESULTS

Equations (1) and (3) are solved in the cases of the boundary layer and the plane jet and provide the downstream variations of $\overline{\theta'^2}$, ϵ_{θ_x}, ϵ_{θ_y} and ϵ_{θ_z} (and hence of ϵ_θ) at the source height. Measured values of the latter quantities at the first experimental section are chosen as initial conditions. In the case of the boundary layer, the mean velocity $\overline{u}$ in Eqs. (1) and (3) is constant and equal to 5 m.s^{-1}. In the case of the plane jet, it decreases from 6 m.s^{-1} to 4.8 m.s^{-1} in the investigated region. As regard to constant values, $\psi_\theta = 3.3$ (close the above derived value 10/3) and $\alpha_{\mathcal{R}} = 4$, for the case of the boundary layer. Note that the evolutions of $\overline{\theta'^2}$ and ϵ_θ are insensitive to $\alpha_{\mathcal{R}}$. The value of the latter is chosen so that the model predictions fit the experimental ϵ_{θ_x}, ϵ_{θ_y} and ϵ_{θ_z} which gives an estimation of the return-to-isotropy timescale. In the case of the plane jet, however, the experimental data have been found to be better fitted with slightly different values namely, $\psi_\theta = 2.8$ and $\alpha_{\mathcal{R}} = 3$. This could be explained by the fact that, in the plane jet, the budget of temperature variance at the source height does not exactly amount to a convection/dissipation equilibrium (Rosset, 2000). Moreover, the equivalence between a continuous line source and an instantaneous area source used for deriving ψ_θ (see above) can be questioned in the case of the plane jet because of the rather large turbulence intensity at the source location (table 1).

In Figs. 3 to 8, the downstream distance is rescaled as $x^\star = \sigma_{vs}x/U_s$ which is proportional to the mean width of the thermal sheet; σ_{vs} is the root mean square of the transverse velocity at the source location. In Figs. 3, 4, 5 and 7, T_r is a temperature reference based on the heating power.

The decay of temperature r.m.s in the boundary layer and the plane jet is reported in Figs. 3 and 4 respectively. In the boundary layer, this decrease follows approximately a $x^{-0.75}$ law and is rather well described by the model which confirms that the 'theoretical' value $\psi_\theta = 10/3$ is suitable to this situation. In the plane jet, the experimental data display a $x^{-0.75}$ decay up to $x^\star = 2.5$mm and, afterwards, an evolution closer to x^{-1}. The model underestimates the r.m.s in this latter phase.

Predictions of ϵ_{θ_x}, ϵ_{θ_y} and ϵ_{θ_z} as well as of the return to isotropy represented by the decay of $\epsilon_{\theta_y}/\epsilon_{\theta_x}$ and $\epsilon_{\theta_z}/\epsilon_{\theta_x}$ have been found acceptable in the boundary layer (Figs. 5 and 6) provided that $\alpha_{\mathcal{R}} = 4$. This implies a return-to-isotropy time scale $\tau_{\mathcal{R}} = 0.5\tau_\theta$. Figure 7 displays the contributions to temperature variance dissipation in the plane jet. Here, $\alpha_{\mathcal{R}} = 3$ and thus $\tau_{\mathcal{R}} \simeq 0.67\tau_\theta$, not so far from the value derived in the boundary layer. The rather high initial level of anisotropy deserves to be mentioned. In the boundary layer, $\epsilon_{\theta_y}/\epsilon_{\theta_x} \simeq 30$ and $\epsilon_{\theta_z}/\epsilon_{\theta_x} \simeq 1.6$ at the first experimental section. In comparison, values as high as $\epsilon_{\theta_y}/\epsilon_{\theta_x} \simeq 78$ and $\epsilon_{\theta_z}/\epsilon_{\theta_x} \simeq 6.6$ have been measured in the plane jet.

The longitudinal evolution of the temperature microscales in the boundary layer is shown in Fig. 8. These are defined as $\lambda_{\theta_x}^2 = 2\overline{\theta'^2}/\overline{(\partial\theta'/\partial x)^2}$ etc. The significant feature is the minimum in the evolution of λ_{θ_x} and λ_{θ_z}. A similar behaviour has been found in the plane jet. It is likely that, in the first stage, the thermal sheet experiences corrugations along both the longitudinal and spanwise directions under influence of small-scale vorticity which results in a decrease of the temperature microscales in these directions. This trend is retrieved by the model, at least qualitatively, through the predominance of the return to isotropy in the early evolution of ϵ_{θ_x} and ϵ_{θ_z}. As a matter of fact, in the model, the initial small values of the latter quantities cause their relaxation term (second on right-hand side of Eq. (3)) to be large and positive; this counteracts their decay due to isotropic dissipation and implies a minimum in the microscales since $\lambda_{\theta_x}^2 \propto \overline{\theta'^2}/\epsilon_{\theta_x}$ and $\lambda_{\theta_z}^2 \propto \overline{\theta'^2}/\epsilon_{\theta_z}$.

CONCLUSION

Injection of heat via a small-diameter line source placed in a turbulent boundary layer and a turbulent plane jet has enabled us to directly impose a high anisotropy level at the small scales of a scalar field. Due to the geometry of this injection, ratios $\epsilon_{\theta_y}/\epsilon_{\theta_x}$ as large as 30 in the boundary layer and 78 in the plane jet have been measured. The ratio $\epsilon_{\theta_z}/\epsilon_{\theta_x}$ has also been found larger than unity (1.6 in the boundary layer and 6.6 in the plane jet as larger values). This latter feature might be explained by the fact that the preferential orientation of small-scale vorticity imposed by shear imply a redistribution of the fluctuating temperature gradient which may promote ϵ_{θ_z} at the expense of ϵ_{θ_x} (Diamessis and Nomura, 2000). Further work is needed to understand more precisely how can such a scenario hold in our case.

A significant result is the return to isotropy of temperature dissipation with downstream distance. This is important as regard to the lack of information on this phenomenon. We have shown that the evolutions of ϵ_{θ_x}, ϵ_{θ_y} and ϵ_{θ_z} at the source height, in the region of the thermal field where the temperature variance decay is governed by convection and dissipation, can be rather well described by a model based on a convection/isotropic dissipation/return to isotropy regime. Comparison of model predictions with experimental data has furthermore allowed us to estimate the return-to-isotropy time scale. In the investigated region, this time scale is close to $0.5\tau_\theta$ in the boundary layer and to $0.67\tau_\theta$ in the plane jet, where τ_θ is the scalar time scale, $\overline{\theta'^2}/2\epsilon_\theta$. Reasonable model predictions are however more difficult to obtain in the case of the plane jet.

This study has shed some light on the return to isotropy of the scalar dissipation. Although it can be suspected that both stretching (probably via the action of vorticity) and molecular dissipation play a role in this process, the complete scenario remains to be depicted.

REFERENCES

Aronson, D., and Löfdahl, A., 1993, "The Plane Wake of a Cylinder: Measurements and Inferences on Turbulence Modeling", *Physics of Fluids A*, Vol. 5-6, pp. 1433-1437.

Diamessis, P. J., and Nomura, K. K., 2000, "Interaction of Vorticity, Rate-of-Strain, and Scalar Gradient in Stratified Homogeneous Sheared Turbulence", *Physics of Fluids A*, Vol. 12, pp. 1166-1188.

Dumouchel, F., Lecordier, J. C., and Paranthoën, P., 1998, "The Effective Reynolds Number of a Heated Cylinder", *International Journal of Heat and Mass Transfer*, Vol. 41, pp. 1787-1794.

Fall, A., 1997, "Contribution à l'Etude du Micromélange en Ecoulement Turbulent au Voisinage de Sources Pariétale et Ponctuelle. Application au Cas Réactif", Ph.D. Thesis, University of Rouen.

Gonzalez, M., 2000, "Study of the Anisotropy of a Passive Scalar Field at the Level of Dissipation", *Physics of Fluids A*, Vol. 12, pp. 2302-2310.

Krishnamoorthy, L. V., and Antonia, R. A., 1987, "Temperature-Dissipation Measurements in a Turbulent Boundary Layer", *Journal of Fluid Mechanics*, Vol. 176, pp. 265-281.

Pumir, A., 1994, "A Numerical Study of a Passive Scalar in Three Dimensions in the Presence of a Mean Gradient", *Physics of Fluids A*, Vol. 6, pp. 2118-2132.

Raupach, M. R., and Legg, J. E., 1983, "Turbulent Dispersion from an Elevated Line Source", *Journal of Fluid Mechanics*, Vol. 136, pp. 111-137.

Rosset, L., 2000, "Etude Expérimentale et Modélisation de l'Evolution de la Structure d'un Panache dans un Ecoulement Turbulent Inhomogène", Ph.D. Thesis, University of Rouen.

Rosset, L., El Kabiri, M., Paranthoën, P., Gonzalez, M., and Lecordier, J. C., "Equation de Bilan de la Variance des Fluctuations de Température en Aval d'une Ligne Source de Chaleur Placée dans un Ecoulement Turbulent", *Proceedings, Congrès Français de Thermique, SFT 2000*, Elsevier, pp. 157-162.

Sreenivasan, K. R., 1991, "On Local Isotropy of Passive Scalars in Turbulent Shear Flows", *Proceedings of the Royal Society of London*, Vol. 434, pp. 165-182.

Sykes, R. I., Lewellen, W. S., and Parker, S. F., 1984, "A Turbulent-Transport Model for Concentration Fluctuations and Fluxes", *Journal of Fluid Mechanics*, Vol. 139, pp. 193-218.

Thomson, D. J., 1997, "Eulerian Analysis of Concentration Fluctuations in Dispersing Plumes and Puffs", *Physics of Fluids A*, Vol. 9, pp. 2349-2354.

Tong, C., and Warhaft, Z., 1994, "On Passive Scalar Derivative Statistics in Grid Turbulence", *Physics of Fluids A*, Vol. 6, pp. 2165-2176.

Warhaft, Z., 2000, "Passive Scalars in Turbulent Flows", *Annual Review of Fluid Mechanics*, Vol. 32, pp. 203-240.

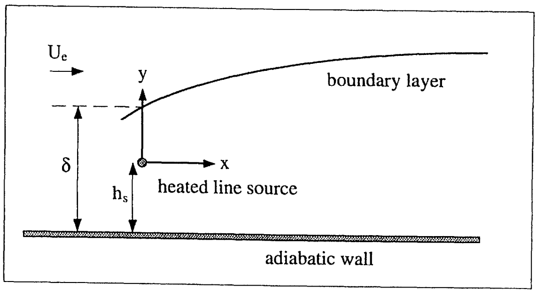

Figure 1: Experimental device in the boundary layer.

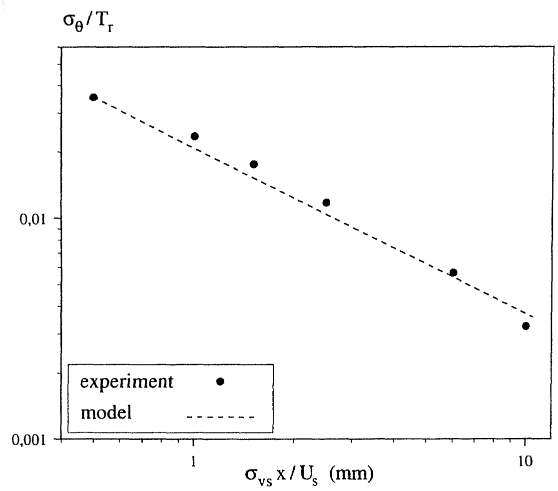

Figure 3: Decay of temperature r.m.s in the boundary layer (at the source height).

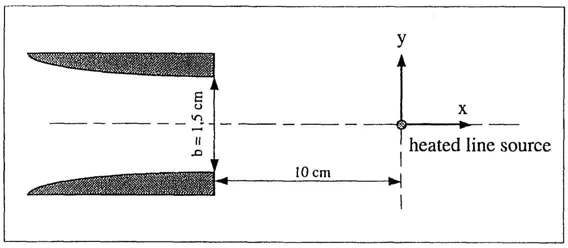

Figure 2: Experimental device in the plane jet.

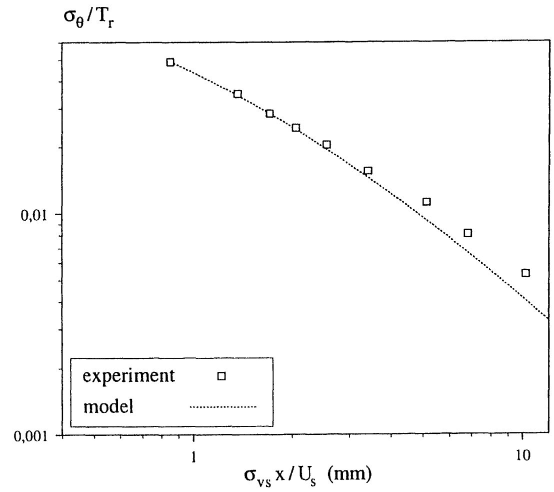

Figure 4: Decay of temperature r.m.s in the plane jet (at the source height).

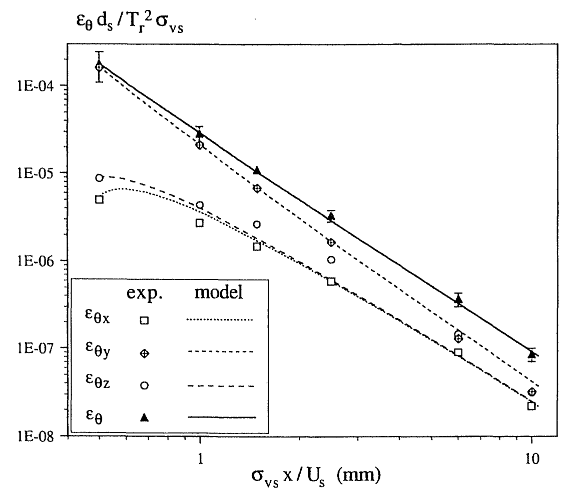

Figure 5: Dissipation of temperature variance in the boundary layer (at the source height).

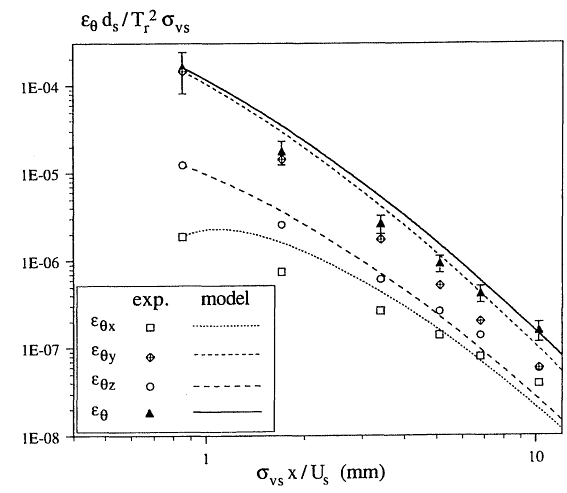

Figure 7: Dissipation of temperature variance in the plane jet (at the source height).

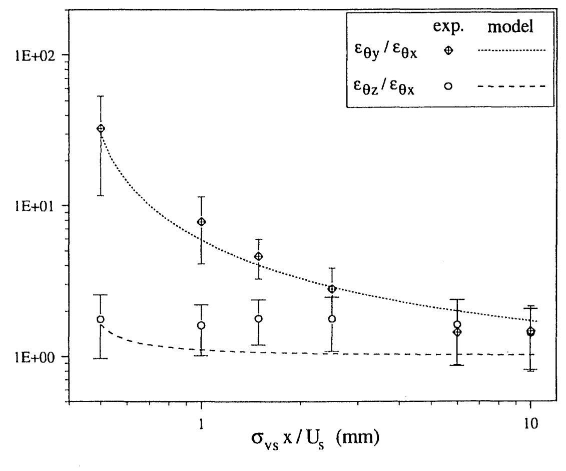

Figure 6: Return to isotropy of temperature dissipation in the boundary layer (at the source height).

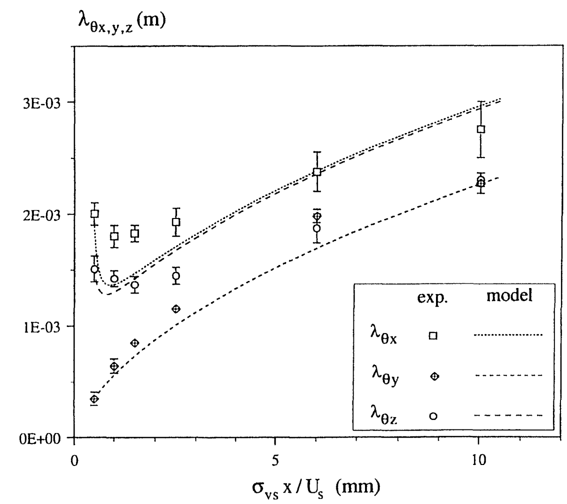

Figure 8: Temperature microscales in the boundary layer (at the source height).